Application of Thermal Barrier Coatings on Combustion Chamber Liners – A Review.

B. Goswami, S.K. Sahay*, and A.K. Ray,

National Metallurgical Laboratory, Jamshedpur, India, and (*) Department of Metallurgy and Materials Science, National Institute of Technology, Jamshedpur, India

(Received February 6,2004; final form April 1,2004)

ABSTRACT

Thermal barrier coatings (TBC) help to reduce the temperature of combustion chamber liner by 473-573K during operation on being aided by swirls of film cooling air. Versatility and low production cost make air plasma spray (APS) TBCs more attractive on liners. However spinal formation at the top to bond coat interface induces ceramic sintering rate and forms thermally grown oxide (TGO) growth. Lifing of engines is attempted to utilize existing design and remnant life within design constrains by giving emphasis on coating philosophies. A proper and efficient substitute with multimetallic bond coat and ceramic topcoat yields longer hours of exposure. Parallel removal of harmful elements in the liner material, restriction on the use of poor quality fuels, and atmospheric effects increase life. Studies of remnant life assessment have been found to be based on control of parameters that check TGO growth, increase adhesion of thicker TGO and restrict ceramic top coat sintering. For example, ceria or lanthana stabilized zirconia transform at comparatively higher temperature than yttria stabilized zirconia.

The current scenarios of protection have been changed to replacements by continuous fiber ceramic composite (CFCC), and ceramic matrix composites (CMC) component, e.g. Sylramic, Nicalon, Naxtal, and Ceraçurb. Non-destructive examination of ceramic translucence based on Parker's optical property produces in-situ information about ceramic degradations.

Keywords: Thermal barrier coating, Combustor liner, Spallation, Emission, Thermally grown oxides, Remnant life, Cooling, Ceramics.

INTRODUCTION

In the last two decades, a conscientious effect has been made to improve the life performance and efficiency of the engines operating at a temperature beyond their melting point through application of thermal barrier coatings on combustion chamber liners. This paper deals with the application of thermal barrier coatings on combustion chamber liners. It also includes the behavior and response of thermal barrier coatings exposed to hostile environments, which prevail on combustion chamber liners. Recent developments in the area of thermal barrier coatings have also been introduced. The central theme of the paper has been to include the maximum scope of application of thermal barrier coating on combustion chamber liners in a fairly comprehensive way. The aim of writing this paper is not only sifting and sorting facts and information from the literature and many excellent texts on the specialized topic but to present the facts and figure in a coherent and comprehensive way. Emphasis has been placed on understanding and exploring the atomistics of flow and

fracture of thermal barrier coatings under the diverse and complex high temperature phenomena. An attempt has been made to give detailed consideration of mechanisms of high temperature deformation of thermal barrier coatings. A comprehensive treatment on the application of thermal barrier coatings has been dealt so as to stimulate the interest in this growing area of research. Adequate references have been given on various aspects of thermal barrier coatings to point out derivations or analysis beyond the scope of this paper. These references provide key to the further information on many controversial points, which are beyond the breadth and scope of the paper.

Design and development of combustion engine varies with the temperature profile of the system. The key temperature profile formers are high temperature components such as combustion chamber liner (or combustor liner). The fuel is combusted and the flame is augmented over liner within primary and secondary (coolant) airflow from compressor. The requirement of higher turbine inlet pressure is to produce adequate temperature and pressure correlation from proportion of excess secondary air, which is introduced. The parallel requirement of low oxides of nitrogen (NO_x) emission restricts combustion temperature. Subsequent high liner metal durability is obtained by reducing coolant air reaction quenches to liner metal respectively. To reduce combustion temperature for low NO_x, a design modification of enlarged liner diameter becomes essential for carbon monoxides (CO) reduction in exhaust. The liner coating reduces marginal temperature increment and variation of metal temperature /1/. Improvement in combustion performance response to fatigue, creep, and stress rupture properties is primarily subtractive due to reduced thermal-mechanical load variations of combustor. Combustion chamber load variations arise as a result of combustion oscillations, flame temperature variation, particularly during start up schedules. Combustion chamber oscillations increase for low NO_x dry emission modifications. Increasing combustor volume (diameter only) and liner diameter reduces it within existing design constrains. Thus premix lean combustion reduces liner wall temperature fluctuation in augmented backside cooling (ABC) liner more than in louvered or effusion cooled liner /2/. The combustion temperature of 2200K is reduced by secondary air to 1089K in the environment and liner temperature from turbine firing temperature of 1393K to 1173K. The liner inner wall (ABC modification) is uncoated which acts as a quite steady temperature-cooling surface. The outer wall is coated to reduce thermal fatigue arising as a result of inflamed combustion of fuel. Ceramic coatings are used on combustor liners and hot section components of turbine to protect substrate from heat penetration and associated variation /3,4/. The liners are passages of combustible gases for completion of combustion and subsequent reduction of hot gas temperature by secondary air. The temperature reduction up to a tolerable limit increases the life of liner metal /5-7/. This approach also establishes one of the lifing methodologies of remnant life estimation. Liner life increases when a swirl of air passes at the vicinity of coated surface, so that uniformity of thermal gradient remains within control through a cooling air blanket. It also reduces the contact of corrosive gases with ceramic coating. Ceramic coating is refractory metal oxide and immune to further oxidation. However, combustible gases permeate through the intergranular pore and void profiles. These subsequently react to bond coat and adversely affect its performance in service /8-10/.

Thermal barrier coatings lose their properties with increasing time of exposure /11-16/. Therefore life prediction is an important task in studying their phenomenological physical-thermal-chemical-mechanical processes /17-26/. To reduce the failure possibilities thermal barrier coating protects best on liners of modern combustion chamber made of nickel base superalloys. The history of protection from mainly corrosion to both insulation and corrosion has been developed from metallic cementation coatings to air plasma spray thermal barrier coatings (APS TBC) and electron beam physical vapor deposition (EB PVD) techniques /27-29/. The development of fine-grained columnar deposition with 10-25% voids and pores by later processes insulates metallic substrate at appreciable structural compliance tolerances. The low adherence and corrosive gaseous-permeation properties of ceramic coating are accepted after design of the bond coat layer within the substrate and ceramic coating /30/. The improved version of functionally graded materials (FGM) coatings from totally metallic to totally ceramic

constituent lowers interfacial mismatch characteristics, a novel approach to improve the life. The physical-thermal-chemical-mechanical phenomenon undergo complex interactions at the composite state of interface on various times of exposure in service /31,32/.

The interfacial bondings in usual cases of APS TBC's on APS BC's (bond coat) and subsequently over nickel base superalloys are mostly mechanical-chemical bonding and totally chemical-metallurgical bonding respectively. The ceramic to metallic bond coat interfacial is mostly adhesion bonding. This interface bears most of the failure possibilities. The response of aging of implement is seen at the interface in terms of different oxidized constituents. The valuable element depletion at the bond coat produces the effect of aging. However, lifing methodologies depend on control of mainly diffusing species by restricting contamination either indigenously or exogenously. The indigenous contamination arises from those materials which are used for fabrication /33/, while exogenous materials contaminate from atmosphere of combustion. These may be through compressor air or through combustible product constitutions /34,35/. Introduction of continuous fiber ceramic composite (CFCC), ceramic matrix composites (CMC), environmental barrier coating (EBC) on ceramic components and TBC coated components to liner application appears to perform better than conventional systems. However, limitations have arisen from temperature and corrodant content in the system. Non-destructive test/examination (NDT/E), on these systems based on optical phenomenon and residual stress measurements of thermally grown oxides (TGO) at interface produce improved exploratory information /36/.

This paper is presented to correlate simulated approaches with practical deficits. The aim is to produce relative activity of cooling methodology and remnant life assessment to the liner.

Thermo-mechanical and thermo-chemical phenomena are complex and diverse in nature in thermal barrier coatings. Hence it becomes a challenging problem to understand them in terms of fundamental principles to achieve the full potential of thermal barrier coatings.

Thermal barrier coatings suffer from problems of spalling and reduced adherence to substrate due to a number of reasons. It is believed that the thermal expansion mismatch across the interface is responsible for such a damaging behavior. Understanding of the complex interplay of phenomena such as diffusion, oxidation, phase-transformation, elastic deformation, plastic deformation, creep deformation, thermal expansion, thermal conduction, radiation, fracture, fatigue, and sintering becomes a challenging opportunity in design and development of thermal barrier coatings. As a result interest in this exotic area has increased dramatically over the past two decades. It is also being reflected from the series of excellent papers and articles available today on this exciting and innovative field of thermal barrier coatings. Active research on the study of the mechanisms of auto sintering of thermal barrier coatings is in progress to explore how to minimize thermal expansion mismatch stresses. It is suggested that the application of composite made from functionally graded materials, micro-laminated, and multilayered ceramics/ceramics or metallic/ceramic or metallic/metallic coatings help to decrease the thermal expansion mismatch stresses.

GAS TURBINE AND COMBUSTION CHAMBER LINERS

A gas turbine engine is an air-dependent thermal jet propulsion device that uses exhaust gas driven turbine wheels to drive the compressor, making continuous operation of the engine possible. In gas turbine engine, a separate section is devoted to each function of intake, compression, combustion, and exhaust. All functions are performed at the same time without interruption. The compressor brings in compresses, and forces air into the combustion section. Fuel is injected into the combustion area, where it mixes with the compressed air. The fuel and air mixture is ignited initially and rendered as self-supporting combustion in the next steps. It is designed to burn a fuel/air mixture and to deliver combusted gases to the turbine at a temperature not exceeding the allowable limits at the turbine inlet. Theoretically the compressor delivers 100% of its air by volume to the combustion chamber. However, the fuel-air mixture has a ratio of 15 parts air to 1 part fuel by weight. Approximately 25% of air is used to attain the

desired fuel-air ratio. The remaining 75% is used to form an air blanket around the burning gases and to dilute the temperature by approximately one half, which otherwise may reach as high as 2200K. This ensures that the turbine section will not be destroyed by excessive heat. The air used for burning is known as primary air and that uses for cording are secondary air. Secondary air is controlled and directed by holes and louvers in the combustion chamber liners. The location of combustion chambers are always arranged co-axially with the compressor and turbine, regardless of type, since the chambers must be in a through flow position to function efficiently. All combustion chambers contain the same basic elements: a casing, a perforated inner liner, a fuel injection system, means of initial ignition, and a fuel drainage system to drain off unburned fuel after engine shut down. A combination of propeller and exhaust jet provides the best propulsive efficiency in aircraft propulsion. A single-shaft turboprop engine (Rolls-Royce Dart) has used a centrifugal compressor and can type combustion chambers in the years between 1953 and 1985 /2/. One of the recent introductions of GE 90 in airways sector comprises a combustor with the following features. The combustor is aero-thermo tuned (for power setting) dual dome annular in design. Improved operability has been attributes of long-life liner construction, and reduced NO_x, unburned hydrocarbon, carbon monoxide, and smoke levels /37-39/.

COMBUSTOR LINER AND COOLING-DESIGN METHODOLOGIES

A combustion chamber is a hot gas path component. Combustor wall temperatures can be very high. The materials undergo very abrupt temperature changes on start and stop, so that low cycle fatigue is an important failure mode. Steady state thermal stresses can also be significant due to the nature of the combustion process. A design that is flexible but still able to withstand thermal fatigue is a must. The combustion process itself generates high frequency vibration, which can result in high cycle fatigue (HCF) failure /40,41/. The relatively thin walls of the combustor can and liner mean that oxidation is also an important failure mode. Finally the pressure outside the combustor is somewhat higher than the inside. Since the walls are thin, this pressure difference is sufficient for creep rupture and buckling, where temperature is the highest. For GE engines the materials that have been used in the construction of combustor are the nickel-based alloys, such as hastelloys-X, RA333, and nimonic 263.1. Thermal barrier coatings are widely used to maximize the effects of external cooling air, maintaining metal temperature within creep limits and helping to mitigate thermal gradients. These are usually around 254μm of plasma sprayed yttria stabilized zirconia, with a bond coat of plasma sprayed NiCoCrAlY. Coatings based on aluminide intermetallic phases are brittle at low temperature and ductile at high temperature. The temperature at which the changes take place is called ductile to brittle transition temperature (DBTT). It is important that the DBTT should be as low as possible, so that cracking in the coating does not occur in service. With turbine firing temperatures exceeding 1393K and thereby challenging the ability of air cooling to maintain surface temperatures below about 1173K, there has been a very considerable growth in the use of thermal barrier coatings. The function of the thermal barrier is to retard the conduction of heat from the combustion gas to the inlet cooling air, and thus either reduce cooling air needed, or allow an increase in the turbine inlet temperature for a given metal temperature. Air plasma spray yttria stabilized zirconia of 125-375μm thick is coated over MCrAlY bond layer of 75-125μm thick to reduce metal surface temperature and to smooth out hot spots. Thus thermal barrier coating reduce thermal fatigue stresses of combustion section (combustor cans/liners and transitions) of newer models /42-47/.

The objective of design robustness is to find settings for design parameters, which will not only maximize performance, but also minimize the influence of uncertainty on performance. This methodology is formulated as a general approach to any uncertain design. The simulation is applied to the design of a combustion chamber liner in order to quantify the effect of cycle parameter and heat transfer coefficient uncertainties on combustor liner metal temperature variance. The results show that for the parameter ranges of interest, impingement hole spacing and thermal barrier coating has the greatest effect on metal

temperature variance. Uncertainty in design is inability to predict the exact value of a design parameter that affects the performance of a system. Uncertainty arises from the evolution of a design as it progresses from conceptual to detailed phases. The idea of uncertainty provides means of grouping design parameters into two categories: control parameters and noise parameters. Control parameters are variables that the designers have direct control over, while noise parameters are variables that affect the design, but are beyond the designers' control. Noise parameters should be specified probabilistically in terms of a range and probability distribution. The goal of robust design is to minimize the influence of uncertainties such as atmospheric conditions on the performance of the design.

Liner cooling design is to keep the liner peak metal temperature below some maximum metal temperature set by the strength and material considerations, using the smaller cooling mass flow rate possible. The designer needs a way of minimizing the effect of uncertainty in such a manner as to be reasonably assured that liner temperature limitations will not be exceeded regardless of flight condition, ambient temperature, manufacturing imperfections and so on. The model describes steps of cooling design methodology. The central element is an analysis tool that is capable of predicting the peak liner metal temperature as a function of cooling geometry, liner flame side boundary conditions, and liner back side boundary conditions. Backside boundary conditions are calculated through cycle analysis and cooling analysis. Cycle analysis is used to calculate coolant temperature while cooling analysis is used to calculate backside heat transfer coefficient. Typically, this cooling analysis is based on a regression of experimental data for the cooling configuration under consideration. Flame side (or gas side) boundary conditions are more difficult to calculate because flame side flow patterns are usually not uniform. Those zones near a swirled cup are subject to intense flame scrubbing, which creates hot spots in the liner metal, where guesswork is task to calculate radiative heat flux into the liner wall. The liner thermal model constitutes a model for liner metal temperature as a function of cycle parameters and cooling system geometry. In an abstract sense, one thinks of the liner cooling model as a black box, which takes cooling geometry and cycle information and returns a liner metal temperature. Quick and accurate estimation for liner metal temperature is creating a model of Response Surface Methodology (RSM). It uses design of experiments (DoE) to create a set of simulations, which are run to find a response, for liner temperature. Subsequently these simulations are used to derive a polynomial equation for liner metal temperature as a function of liner geometry and engine cycle variables. This response surface equation (RSE) is used in place of detailed liner model to perform the Monte Carlo Simulation (MCS). Over all evaluation criterion (OEC) is product of mean and variance. Minimization of OEC leads to a solution with minimum variance and mean temperature. Pareto plot of OEC equation describes TBC thickness and hole spacing are most dominating parameters. The lowest liner temperature will occur for the minimum hole spacing ($\frac{x}{D}$ = -1), maximum TBC thickness (+1), maximum impingement baffle pressure drop ($\frac{\Delta P}{P}$ = +1), and minimum hole diameter (D = -1). Where ($\frac{x}{D}$, $\frac{Z}{D}$, D) = impingement geometry parameters, T_{flame}, T_{cool} = engine cycle parameters, $\frac{x}{D}$ = non-dimensional impingement hole spacing, $\frac{Z}{D}$ = impingement gap spacing, D = impingement hole diameter, h_{gas} = flame side convective coefficient, k = liner metal thermal conductivity, $\frac{\Delta P}{P}$ = impingement baffle pressure drop, TBC thickness = Thickness of TBC on the flame side of liner, T_{flame} = adiabatic flame temperature, T_{cool} = Coolant temperature impinging on the liner back side, where $\frac{x}{D}$, $\frac{Z}{D}$, D, K, $\frac{\Delta P}{P}$, TBC thickness are control parameters, and T_{flame}, T_{cool}, h_{gas} are noise parameters /48/.

POLLUTANT EMISSIONS AND ADVANCED COMBUSTOR LINERS

Awareness of pollutant problems from combustion smoke has focused attention on the design and development of high efficiency combustors. Oxides of nitrogen (NO_x) formation are affected by flame temperature. Theoretically they are at a maximum at stoichiometric conditions and fall at both rich and lean mixtures. Reductions of NO_x by operating well away

from stoichoimetric conditions result in formation of both carbon monoxide (CO) and unburned hydrocarbons (UHC). The rate of formation of NO_x varies exponentially with flame temperature, while a slight dependence is found on the residence time of the fluid in the combustor. Axially staged combustion is developed to result in a longer combustion than annular arrangement. The staggered inline arrangement reduces length penalty and has greater potential for emission reduction. General Electric has designed a multiple combustor for heavy industrial gas turbines. The design is based on modification of cans. The original can had a single burner, but a ring of six primary dual-fuel burners surrounding a single secondary dual-fuel burner has replaced this. The convergent-divergent section of primary zone and venturi of secondary zone respectively accelerates the flow and stabilizes the flame by re-circulation /2/.

Modifications of liner design are based on either pollution control requirements or are specific to the implementation /48-49/. For example, environmental legislation requires lean premix combustor liners (Dry low NO_x gas turbines (DLN, GT's)), HSCT aircraft require robust combustion chamber liners, and heavy duty liners are required for power plants /48-50/. The following description states some of the modifications in brief.

(1) Lean premix airways sector combustor liner: - Lean-premix combustion reduces conversion of atmospheric nitrogen to NO_x by reducing combustion flame temperature. Since NO_x formation rates are strongly dependent on flame temperature. Premixing the fuel and combustor airflow upstream of the combustor primary zone enhances lean combustion. Premixing prevents local hot spot within the combustor volume that can lead to significant NO_x formation. The three aspects of lean-premix combustion are CO/NO_x trade off, combustor operating range, and combustor pressure oscillations. The CO/NO_x trade off involves combustion air control at primary zone and increase in combustor volume by diameter. As the operation moves away to part load, the operating range aspect is to be solved by variable geometry or compressor air bleed. The combustion pressure oscillation is a result of lean-premix combustion can lead to engine damage. The third aspect is recovered by the use of air swirls of the fuel injectors. Part cooling and dilution air may be used by either louvers on the inside of the liner to form protective cooling air film or commercial diffusion cooling or back side cooled liners. The backside cooling requires no cooling air injection. The augmented backside cooling (ABC) liner is considered to be the most advanced because it neither forms reaction quenching to produce CO, nor increases NO_x level. An application of thermal barrier coating protects hot surface of liners of ABC type, while the modern trend replaces the coated metallic liner to ceramic liners, where cooling air injection is avoided in addition to emission limitations /1,49/.

(2) Ultra-lean premix airways sector combustor liner: - The Mercury 50's ultra-lean premix design is a further refinement of solar's successful $SoLoNO_x^{TM}$ technology. It has a back-side-cooled annular combustor liner and closed-loop carbon monoxide (CO) feed back control to achieve single-digit NO_x emissions at 50-100% load range. Lean to ultra-lean combustion is the usage of additional dilution air through injector body to reduce primary zone. The zone temperature is maintained consistent with load. The proportional air injection under effectively modulated variable geometry of design produces compensating nature among pressure drop across combustor at lower loads, bleed air, and lean operation for a wide range of load. The CO transformation of lean combustion cools liner instead of cooling air. However low temperature combustion reduces NO_x, and increases CO in gas. Minimizing both CO and NO_x a balance of temperature is applied. Alternative liner cooling scheme is referred to augmented backside cooling. This maintains higher wall temperature as compared to lower or effusion cooling technique to further retard the formation of CO during combustion. This in turn allows the reduced primary zone temperature necessary for single digit NO_x without sacrificing an increase in CO emission. A ceramic thermal barrier coating (TBC) that is plasma sprayed to the metallic substrate protects the combustor liner. The addition of trip strips to the backside of liner serves to break up the boundary layer and promotes improved heat transfer. Liners manufactured from continuous fiber reinforced ceramic composite (CFCC) design are in an advanced stage for application /34/.

(3) Robust high-speed civil transport (HSCT) combustor liner: The desire for faster and high flying supersonic has raised concerns about the effect on the earth's atmosphere. Emissions of nitrogen oxides (NO_x) are known to act as catalysts for the decomposition of ozone in the ozone layer. Two of the most promising low emission combustors are the rich-burn, quick-quench, lean-burn (RQL), and lean, premixed, pre-vaporized (LPP) combustors. NO_x production is reduced at lower combustion temperature. The RQL and LPP combustors use different approaches to reduce combustion temperature. The RQL combustors use a staged combustion technique while the LPP combustor depresses flame temperature by burning a lean fuel-air mixture. The following description states LPP simulated design in brief. LPP combustor liner cooling characteristics are considered to be more important, because effective air for cooling purpose is less. In conventional combustors almost 50% air is by-passed around the combustion region and used for dilution and cooling. The LPP combustor maintains a low flame temperature by burning the fuel-air mixture at lower than stoichiometric (lean) conditions. In effect, the flow in the combustion region contains more air than is needed to completely combust all of the fuel in the combustion region. Thus, the remaining air acts as a diluent, which cools combustion by-products to an intermediate temperature, thereby inhibiting NO_x formation. Thus the requirement for lowered NO_x emissions levels results in difficulties of cooling the combustion internal part, particularly the liner.

The HSCT robust liner is an impingement cooled singled combustor liner. The liner consists of three segments, each of which is impingement cooled. Combustion air passes through the pre-mixer into the flame and outer passages and through the impingement baffle. After impinging on the liner backside the spent air is exhausted into the high-pressure turbine gas stream. Impingement cooling provides effective cooling at a low coolant mass flow rate. This uses a perforated plate (impingement baffle) to direct jets of cooling air onto the liner backside. The result is a high average convective heat transfer coefficient relative to other methods of liner cooling. The average backside heat transfer coefficient is derived in terms of hole diameter Raynold's number (ReD), hole diameter (D), non-dimensional hole spacing (x/D), gap spacing (Z/D), and flow cross section. The maximum metal temperature is modeling coated liner piece between two impingement points. 2-D plane thermal element in ANSYS 5.1 has a three-layer (166 elements) material with a metal substrate on the coolant side and thermal barrier coating (TBC) material on the flame side. A thin layer of bond coat, which is used to bond the TBC to the metal, separates these layers. Obviously the peak metal temperature will occur on the side nearest to the flame and thus the node temperature at the metal bond coat interface is of interest. Assuming sides as adiabatic, this FEM is effectively a 1-D thermal model for liner temperature /48/.

(4) Rich quench lean (RQL) industrial sector combustor liner: The design is to lower conversion of fuel bound nitrogen (FBN) to NO_x in heavy-duty gas turbine of power sector. Rich quench lean combustion decrease conversion of FBN to NO_x because a large fraction of the FBN is converted into non-reactive N_2 in a fuel rich stage. Additional air, requires for complete combustion, is added in a quench stage. A lean stage provides sufficient residence time for complete combustion. The pressure vessel containing combustor is divided into two separate chambers that are fed by independently controlled air supplies. The hot combustion gases flow through the combustor, an impingement cooled transition piece, a sector from the film cooled first stage nozzle of a GELM 6000 gas turbine, and then exit into a water-cooled exhaust duct. Flow visualization tests and computational fluid dynamics (CFD) analyses have shown that the converging section is necessary to prevent the low-pressure core of the swirling flow from drawing lean stage gases back upstream into the rich section. The converging section also provides a convenient method of reducing the flow area to a reasonable size for proper quenching. Rich stage liner is relatively large, but relatively little air is available for cooling. Film cooling, one of the most effective methods of combustor liner cooling is not desirable on the rich stage if NO_x emissions are to be minimized. For these reasons RQL-2 (rich stage combustor liner) is fabricated with a double walled structure. A narrow internal cooling passage conducts cooling air circumferentially around the liner (Figure 1). Air enters each rectangular cooling channel through an inlet hole

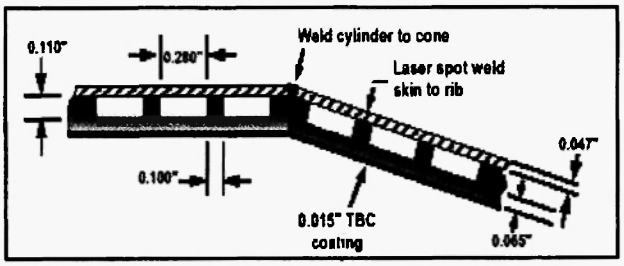

Fig. 1: Double-walled rich stage combustor liner cross-section in the region of the junction between the cylinder and conical section /39/.

and exits each channel through a slot to discharge into one of the collection tubes. Haynes 230 is selected as the material for construction. The quench/lean stage air enters the combustor through quench air holes located at the down stream end of the cylindrical section. Rapid quenching is achieved with quench air holes of different sizes, referred to here as a "radial stratified quench". Larger holes create larger jets to penetrate into hot gas and mix with flow of centerline zone of combustor, while smaller holes create smaller jets to penetrate and to mix with flow adjacent to the wall. Quench holes are sized using standard correlation for jets penetrating into a cross flow. Both the cylindrical section and backward facing steps are impingement cooled. The design goal is for 70% of quench/lean air to enter the combustor through quench holes, with the remaining 30% entering through the lean stage film cooling holes /39/.

(5) Catalytic combustor liner: Catalytic combustion has been in development for several years. Extensive test results combined with analytical design activities resulted in fully functional catalytic combustion system capable of meeting the stringent project emission targets of less than 3 ppm NO_x. Catalytic combustion system consists of a pre-burner, a fuel/air pre-mixture, a two-stage catalyst module and a homogeneous burn out zone. The pre-burner preheats the air to catalyst operating temperatures. The pre-mixture thoroughly mixes the warm air and fuel prior to entering the catalyst module. In the catalyst module the fuel air mixture is primarily converted in a flameless combustion process. The remaining reaction occurs in the homogeneous burn out zone before the hot product gases enter the turbine. Palladium oxide additions to catalyst module show appreciable reduction of combustion temperature /34,51/. Air and fuel of Mercury 50 design is thoroughly mixed and allowed partially to react in the catalyst bed, when temperatures are kept sufficiently low to avoid damage. Burnout is completed down stream of the catalyst bed, where temperatures are sufficiently low to avoid damage and NO_x formation. Catalytic reduction of fuel at 755K is facilitated by recuperated air temperature of 866K, instead of additional pre-burner. Catalyst cans utilize component geometry to maintain a consistent equivalence ratio across the 50-100% operating range /34/. Adiabatic lean-premixed catalytic combustion has the potential to achieve NO_x-emissions below 5 ppm from natural gas turbines. This profile reduces NO_x formation by 3 orders of magnitude based on activation energy for NO_x formation (75 KCal/mol or 3.14×10^8 J/Kmol) upon lowering combustion temperature from 2773K to 1773K. Sufficient catalytic activity for complete combustion and high thermal stability of catalytic materials are technical issues to minimize temperature rise and reduce sintering/loss of activity of catalysts. Palladium oxide supported on alumina or zirconia produce superior activity in the combustion reaction from unique temperature self-control of the reversible transformation of Pd-PdO equilibrium and low volatility of Pd species. Inexpensive thermally stable catalysts has found to be alumina combined with heteroatoms, such as Sr or La. Low growth rate of [001] direction than plane-wise direction is possible by embedded hetro-atoms on separating mirror planes of spinel like substructure at greater phase transformation temperatures for sintering/loss of activity /51/.

THERMAL BARRIER COATING SYSTEMS

Thermal barrier coatings (TBC) are used to protect a variety of structural engineering materials from corrosion, wear, and erosion and to provide thermal insulation (Table-1).

TBC have a most complex structure and operate in most demanding high temperature environment of aircraft and industrial gas turbine engines /47/. A brief description about coating characterization is written below.

Table 1
The major life limiting factors and potential failure modes for hot gas path components in continuous and cyclic duty machines /41/.

Major life limiting factors	Potential failure modes-hot gas path components	
	Continuous duty	***Cyclic duty***
Fuel	Rupture	Thermal mechanical fatigue
Firing temperature	Creep deflection	High-cycle fatigue
Steam/water injection	High-cycle fatigue	Rubs/wear
Cyclic effects	Oxidation	Foreign object damage
	Erosion	
	Corrosion	
	Rubs/wear	
	Foreign object damage	

(I) Properties of thermal barrier coating (TBC): - Insulation and reduction of metal temperature mitigate the effect of hot streaking or uneven gas temperature distribution of heavy-duty liners in industrial sector. TBCs are divided into classes depending on the bond coat and topcoat thickness. Class B TBCs (0.3556 mm to +/- 0.1010-mm topcoat) are the standard for pre-DLN series combustion chamber liners. Class C coating (0.508 mm to +/- 0.0508-mm topcoat) significantly improves the cooling effect on selected DLN industrial liners /41/.

TBC's comprise metal and ceramic multi-layers, insulate turbine and combustor engine components from the hot gas path stream, and improve energy efficiency and durability of engines. The use of TBC's (100-500μm thick), along with internal cooling of the underlying superalloy component, provides major reductions in the surface temperature (373-573K) of the superalloy. This has enabled modern gas-turbine engines to operate at gas temperatures well above the melting temperature of the superalloy (1573K), thereby improving engine efficiency and performances. The combination of the multi-material nature of TBC structure and demanding operation conditions made TBC more complex than any other coating system. The complexity and severity of TBC structure and the severity of operating conditions are a complex interplay of all of the following phenomena: diffusion, oxidation, phase transformation, elastic deformation, plastic deformation, creep deformation, thermal expansion, thermal conduction, radiation, fracture, fatigue, and sintering. Anatomy of TBC is comprised of four layers made of different materials with specific properties and functions. These layers are substrate, bond coat, thermally grown oxides (TGO), and ceramic topcoat (Figure 2(a) & 2(b)). Substrate is nickel or cobalt based structural superalloy. This is air cooled from inside or through internal hollow channels, thus establishing a temperature gradient across the component wall. The superalloy is investment castings in single or polycrystalline forms, and it contains as many as 5 to 12 additional elements that are added for the enhancement of specific properties such as high temperature strength, ductility, oxidation resistance, hot corrosion resistance, and castability /47/. At the high temperature operation in gas turbine engines, diffusion of elements of high relative concentration can occur between the superalloy substrate and the bond coat. These diffusing elements can occasionally be found in thermally grown oxides (TGO) and the topcoat as well. This inter-diffusion can

Fig. 2(a): Micrograph of the oxidized specimen. Arrow indicates the Al_2O_3 layer of ~2 μm thickness, A – TBC (ceramic layer), B – bond coat, Bo – Al depleted zone, C – substrate /43/.

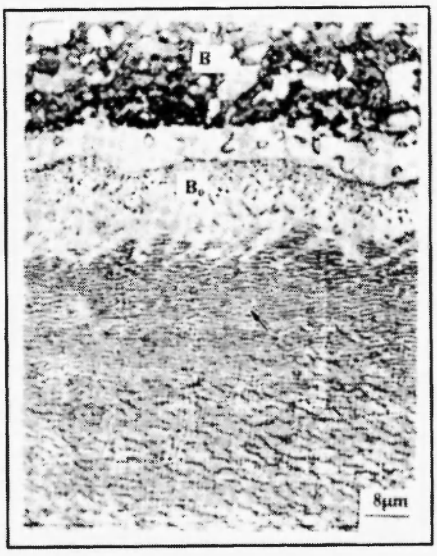

Fig. 2(b): Region Bo is Al depleted zone after the bond coat (region B) in the micrograph of the oxidised specimen. Fraction of Al in the bond coat diffuses into the substrate and builds up a massive γ′ (β-Ni_3Al) phase. The γ′ phase seems to grow laterally in the direction parallel to the bond coat after the Al depleted zone Bo. Arrow indicates the γ ′ phase /43/.

have a profound influence on the spallation failure of the TBC, making it necessary to treat thermal barrier coated superalloys as an engineering system whose properties change with time and cycles during service. The bond coat is an oxidation resistant metallic layer 75-150μm thickness, and it essentially dictates the spallation failure of the TBC. The bond coat is typically made of a NiCrAlY or NiCoCrAlY alloy and is deposited by using the plasma spray or the electron beam physical vapour deposition methods. Other types of bond coats are made of aluminides of nickel and electro-deposited platinum in conjunction with diffusion aluminising or chemical vapour deposition techniques. In minority cases, the bond coat consists of more than one layer, having a different chemical/phase composition. At peak operating conditions the bond coat temperature in gas turbine engines typically exceeds 973K, resulting in bond coat oxidation and the inevitable formation of a third layer the thermally grown oxides (TGO) (1-10 μm thickness) between the bond coat and the ceramic topcoat. The interconnected porosity that always exists in the topcoat allows easy ingress of oxygen from the engine environment to the bond coat. Moreover, even if the topcoat is fully dense, the extremely high ionic diffusivity of oxygen in the zirconia based ceramic topcoat renders it oxygen transparent. Although the formation of TGO is inevitable, the ideal bond coat is engineered to ensure that the TGO forms as alumina and that its growth is slow, uniform, and defect free. Such a TGO has a very low oxygen ionic diffusivity and provides an excellent diffusion barrier, rendering bond coat for further of oxidation. Generally, the inward diffusion of oxygen through the TGO controls further growth of TGO into bond coat, but in some cases TGO growth is controlled by outward diffusion of aluminium, leading to the formation of the new TGO at the TGO/top coat surface or at the alumina grain boundaries within the TGO. Finally the bond coat composition is designed to obtained a highly adherent TGO. It is known that the segregation of sulphur at the bond coat/TGO interface reduces the TGO adhesion dramatically. To mitigate this adverse effect of sulphur, either the sulphur content in the bond coat is maintained below one part per million or sulphur gettering reactive elements (yttrium and zirconium) are added. Other elements that degrade

the bond coat/TGO adhesion (titanium, tantalum) are also kept below acceptable levels in the bond coat, whereas elements that promote adhesion (silicon, hafnium) are added in small quantities /43,47,52/.

The ceramic topcoat layer provides thermal insulation properties that make it the material of choice for the topcoat. It has one of the lowest thermal conductivities at elevated temperature of all ceramics (2.3 W/mK at 1273K for a fully dense material) because of its high concentration of point defect (oxygen vacancies and substitution solute atoms), which scatter heat conducting phonons (lattice waves). YSZ also has a high thermal expansion coefficient (11×10^{-6}/°C or 4.4×10^{-8} /K), which helps alleviate stresses arising from the thermal expansion mismatch between the ceramic topcoat and the underlying metal (14×10^{-6}/°C or 5.13×10^{-8} /K). To further alleviate these stresses, microstructural features such as cracks and porosity are deliberately engineered into the topcoat, making it highly compliant (elastic modulus, 50 Gpa or 50×10^{9} N/m^2) and strain tolerant. YSZ has a relatively low density (6.4 mg/m^3 or 6.4×10^{-6} kg/m^3), which is important for parasitic weight considerations in rotating engine components. It also has a hardness of 14 Gpa or 14×10^{9} N/m^2, which makes it resistant to erosion and foreign body impact. YSZ is resistant to ambient and hot corrosion. YSZ has a high melting point (2973K), making it suitable for higher temperature applications. Although zirconia can be stabilized by a host of different oxides (MgO, CeO_2, ScO_3, CaO), Y_2O_3 stabilized ZrO_2 (YSZ) has been empirically found to be most suitable for TBC application. YSZ-APS-TBC's reduce thermal conductivity of the topcoat from 2.3 W/mK for a fully dense material to 0.8 to 1.7 W/mK within a thickness of 300-600μm. YSZ exists as three different polymorphs- monoclinic, tetragonal, and cubic depending on the composition and the temperature. The addition of 7-8-wt. %Y_2O_3 stabilizes the t-phase, which is most observable phase for TBC applications. This is a variation of the tetragonal phase, but unlike its low Y_2O_3 content (3 mol.% or 3×10^{-3} Kmol%) counterpart, the t-phase does not undergo a martensitic transformation and is therefore more stable. Normally cubic yttria stabilized zirconia systems that exist at room temperature have been 20-wt.% in composition. Interfacial defect density is the main drawback to limiting the period of performance of plasma sprayed implements. However, the simpler solution has been found to be 8-wt.% YSZ. This is not a low yttria equilibrium tetragonal phase, but a phase produced by a diffusionless shear transformation directly from cubic phase and thus contains the full 8-wt.% of yttria. This phase thus contains the full 8-wt.% of yttria (Figure 3).

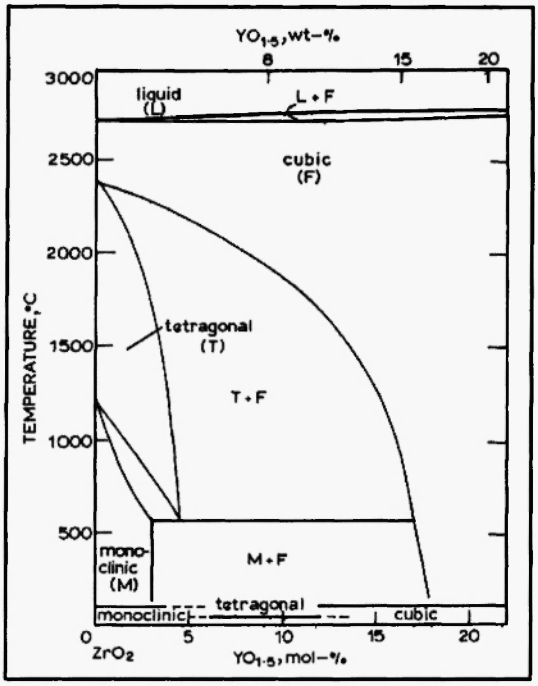

Fig. 3: Zirconia-yttria system, as solid solution /3/.

Heating above 1673K for long periods can decompose this phase. While bulk yttria diffusion and significant grain growth are required to proceed the decomposition. So it is quite stable at the maximum operating temperature comparable to the periods in gas turbines of aero-engine applications /3/. Figure 4(a) and 4(b) shows top view of the spalled coat after cycling at 1323K for 13 cycles of one hour. Undeveloped (Strangemen) microcracks are present in as sprayed condition. These develop and propagate during thermal cycling. Subsequently such defects are available to accommodate imposed strains by free expansion and contraction /95/. Many years of process development establishes EB-PVD and APS-TBC's to be important deposition techniques. APS-TBC's have the following favorable microstructural characteristics. (i) Splat grain morphologies with intersplat boundaries (ii) cracks

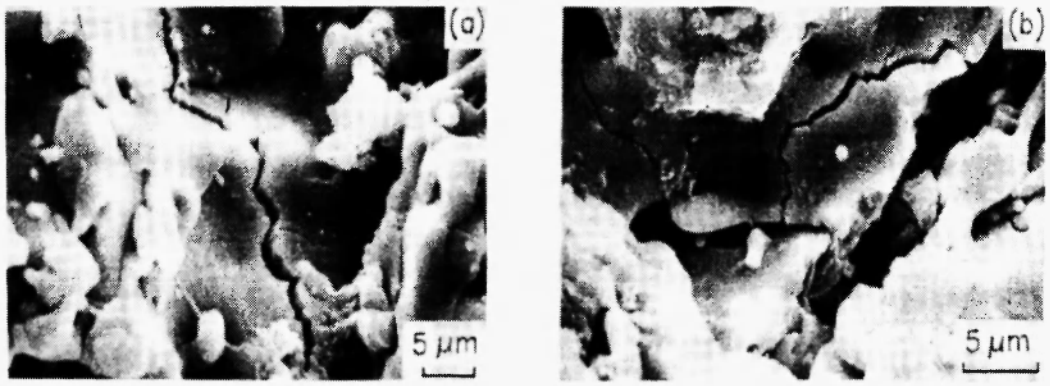

Fig. 4 (a & b): Top view of the spalled top coat after it had been cycled at 1323K for 13 cycles: (a) expansion of microcrack; (b) propagation of microcrack along the solidified columnar structure and collapse of the top coat /24/.

parallel to the metal/ceramic interface for low thermal conductivity and (iii) 15-25% porosity for both low elastic modulus and low thermal conductivity. Figure 5(a) shows air plasma sprayed thermal barrier coating. The basic dynamics of deposit formation have been cohesively bonded splats, which result from high rate impact and rapid solidification of a high flux (millions of particles per cm^2/s) flame melted particles within size range of 10-100 μm.. Inter-splat cohesive strength, size, morphology of porosity, occurrence of crack, defects, and ultra-fine grained microstructure within splats characterize the complex array of entwined splat structure. Splat is flattened out solidification from a molten particle of tens order of micrometer size upon impact with a substrate. The characteristics of splats are affected by temperature of splat, splat viscosity, its surface tension, where as morphology depends on particle velocity, diameter, and substrate surface profile. The main morphology is pancake type and flower type. Figure 5(b) shows three shapes factors defined as below. (a) Equivalent diameter is the diameter of a circle with the same area as the selected feature /4/. (b) Circularity is the elongation of the selected feature, where unity is a perfect circle, and (c) Sphericity is the importance of peripheral material projections at the impact point; where unity is for absence of such projection.

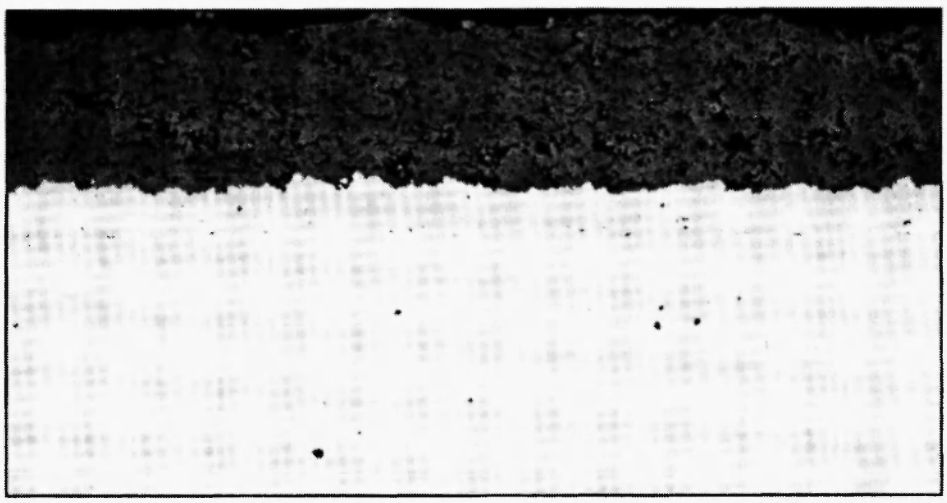

Fig. 5(a): Air plasma sprayed (APS) thermal barrier coating (TBC) /43/.

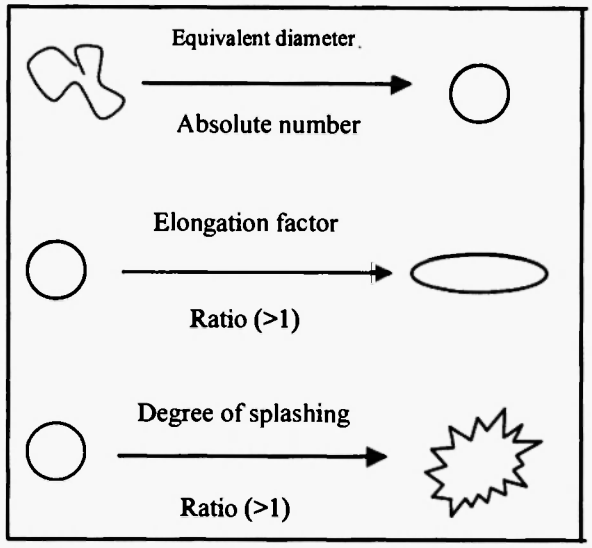

Fig. 5(b): Shape factor associated with formation of a thermal spray splat /4/.

As prepared residual stress has been found to be compressive at the bond coat and tension in the ceramic coat for a system of CoNiCrAlY bond coat and EB-PVD-7Y-ZrO_2 on a hastelloy Y substrate /53/. Samples of YSZ have shown lower removal of as sprayed residual stress. To establish the response of stress removal the samples are annealed at increasing temperatures and then hydrothermally aged at a temperature lower than annealing temperature /54/. The undulating nature of the metal/ceramic interface, which is required for better interlocking adhesion, produces out of phase stresses responsible for in service failure of APS-TBC's as described below. Versatility and low production cost make APS-TBC's attractive commercially. However, deficiencies exist because of the proliferation of microstructural defects parallel to the interface and the roughness of the interface. Comparative thermal cycling experiments have shown low performance of APS-TBC's suitable only for less exacting applications in aircraft engines, such as combustors, fuel vaporizers, and after burner flame holders and stator vanes /11-16/.

Non-rotating components such as combustion chamber can, flare heads, fuel vaporizers, and deflector plates, MCrAlY bonded ceramic systems have shown great benefits.

In these applications even air sprayed nickel aluminide and MCrAlY bond coats with high oxide contents with magnesia stabilized zirconia insulating top coat have shown greater improvements in practice. Internal diameters of combustor cans are sprayed at non-optimum angle. Size variation may preclude bond coat heat-treatment. Table 2 shows composition of typical MCrAlY bonded TBC systems. TBC have failed in service by loss of ceramics and bond coat oxidation, which is improved by application of CoNiCrAlY bond

Table 2
Nominal compositions of some MCrAlY bonded thermal barrier systems, wt.% /22/.

Designation	Bond coat					Ceramics		
	Co	Ni	Cr	Al	Y	ZrO_2	MgO	Y_2O_3
UCAR LTB 4	23	48	17	12	0.3	75	25	---
UCAR LTB 5	22	48	20	9	0.5	75	25	---
UCAR LTB 6	23	48	17	12	0.3	88	---	12
UCAR LTB 7	22	48	20	9	0.5	88	---	12
UCAR LTB 8	39	32	21	7.5	0.5	75	25	---
UCAR LTB 12	39	32	21	7.5	0.5	93	---	6.5
UCAR LTB 13	39	32	21	7.5	0.5	93	---	6.5

coat instead of NiCrAlY and YSZ instead of magnesia stabilized zirconia (MSZ) /22/.

The combustion chambers of some engines have used thermal barrier coatings to reduce metal temperature by 323K. However magnesia stabilized zirconia has limited the performance up to 8000 hours only. Magnesia precipitation at 1223K has been the primary cause of ceramic spallation and sintering. This has been rectified by introduction of 8-wt. % YSZ. This composition has formed a very stable non-equilibrium tetragonal phase during rapid quench of plasma sprayed particles. Primary improvements have been found to be higher fracture toughness and slower rate of crack propagation.

(2) Thermal radiation effects on temperature of thermal barrier coatings: -

Translucent coatings permit energy to be transported internally by radiation. This increases total energy transfer and acts like an increase in thermal conductivity. This degrades insulation ability of coating proportionately with temperature. When a thermal barrier coating is subjected to combustion environment, it is usually covered with a thin layer of shoot. Radiation is then absorbed by shoot, and is partially re-radiated into the coating. In a clean hot coating there is internal radiant emission, absorption, and scattering. Zirconia is somewhat translucent and tends to scatter more than absorb. These modes of energy transfer combine to provide a transport of radiative energy within the coating that acts in combination with heat conduction /55,56/. On the other hand Choy *et al.* /57/ describe the benefits of thermoluminescence to provide smart thermal barrier coatings. Uropium doped thermoluminescence of TBC enables usage as thermographic phosphores to measure temperature at the surface.

(3) Degradation of thermal barrier coatings:

The physical-thermal-chemical-mechanical processes associated with the ceramic-metallurgical system produce marginally enhanced degradation rates /11-16/. Combinations of these phenomena increase complications for an optimum variable selection. Corrosion and oxidation are results of electrical and chemical reactions with other materials. The hot exhaust gas stream encountered in the engine speeds up this reaction. The base alloy determines the degree of oxidation and the properties of the oxide coating formed. If the oxide coating is porous or has a coefficient of expansion different from that of the base metal, the base metal will be continually exposed to the oxidizing atmosphere. One solution to oxidation at elevated temperature is ceramic coatings /39/. Ceramic-coated after burner liners and combustion chambers are in use today. The ceramic coating has two basic functions. (1) Sealing the base metal surface against corrosion, and (2) Insulating the base metal against high temperature. These coatings are not without disadvantages. They are more susceptible to thermal shock. They must have the same coefficient of expansion as the base metal. They are brittle. They have low tensile strength that restricts their use in the engine /33,36,40-43/. Several engine failures have been attributed to thermal shock on the turbine disc. Ceramic coating in particular is vulnerable to this form of stress. Improved fuel controls, starting techniques, and engine design have lessened the problem /33,43/.

TBC's interfacial fracture is assisted by any degradation of the interfacial toughness by fatigue and segregation of undesirable elements to the interface especially sulphur. Sintering within the topcoat at operating temperature that results in the partial healing of the cracks and a reduction in porosity also accelerates TBC failure by making the top-coat less strain tolerant. In addition, sintering increases the thermal conductivity of the coat, resulting in a higher metal surface temperature and the attendant enhancement of bond coat oxidation and creep. It provides thermal insulation and protection from the hot and oxidative combustion gases. Oxides tend to grow with different rate depending on macroscopic surface geometry. Concave surfaces reveal the highest oxide growth rates and convex the lowest growth rates. At 1000 hours and 1273K the difference between the fastest and slowest growing oxide layer is 1μm. At high temperature TBCs (APS-NiCoCrAlY-BC and YPSZ-TC) interfuse the superalloy substrate and the bond coat by outward diffusion of Ni, W, and Cr and inward diffusion of Co and to some extent Al. Fatigue tests are performed to evaluate failure mechanism in TBC systems. The tests include low cycle fatigue (LCF) and thermo-mechanical fatigue (TMF).

Fatigue life is strongly dependent on TGO growth and composition. Adherent alumina layer and long fatigue lives are to be expected. If spinal is allowed to form the fatigue life is strongly reduced and delamination will readily take place /58/. There have been simulated laboratory experiments of the thermomechanical fatigue test (TMF) using in-phase (IP) and out of phase (OOP) stresses. The responses have been evaluated over 7-8 YSZ (CN31) on Pt-Al bond coated (CN91) nickel based single crystal (CMSX4). Susceptibility of coating failure by buckling appears in IP-TMF and crack initiation within bond coat appears in OOP-TMF tests /59/. Thermal fatigue tests have been carried out on YSZ coatings made from sol-gel derived microspheres. The life has appeared to be within 40-50 cycles (30 minutes at 1473K followed by water quench). The as calcined (1273K) microspheres have shown lower monoclinic phases after plasma spray treatment /60/.

Industrial gas turbines (IGT) applications of TBC are long, less cyclic with fewer transients compared with those for aircraft turbine engines. The primary life limiting mechanism is creep rather than thermal fatigue for hot section components. Industrial engines operate in a harsher, less forgiving environment then an aero-engine. TBC is aimed to provide thermal insulation and hot corrosion resistance for a creep life of 25000 hours. Service run ceramic-coated hot section component shows fine particles rich in chromium and sulphur near the bond coat/ceramic coat interface. The effects of contaminant mixture (iron oxide and silica) cause premature failure by respective phase-stabilization and densification. Simulated sulphidation corrosion experiments have been applying thin film (~ 0.5 mg/cm^2 or ~ 0.5×10^{-2} Kg/m^2) of the low melting eutectic mixture from ternary system $MgSO_4$-Na_2SO_4-$CaSO_4$ (with minor additions of K_2SO_4) on component surfaces at a temperature of 1023 and 1173K. TBC degradation in corrodant (Na_2SO_4 + Fe_xO_y + SiO_2) at 1311K for 1000 hours has the following mechanisms Eq^n. No.: 1-3, (Figure 6(a), and 6(b)).

Bond coat degradation:

$Na_2SO_4 + Al_2O_3 + 4\ Ni = 2\ NaAlO_2 + NiS + 3NiO$ (1)

Ceramic degradation:

$Na_2SO_4 + ZrO_2\ (Y_2O_3)(PSZ) = NaYO_3 + ZrO_2$ (Monoclinic), (2)

$ZrO_2\ (Y_2O_3)(PSZ) + Fe_xO_y + SiO_2 = Sinter$ (3)

The long-term experiment has resulted in complete penetration of the contaminants to the bond coat, the formation of porosity and major crack propagation within the bond coat, and ultimately spallation of the entire TBC (Figure 6(c)). The ceramic-coated surface is modified for aerosector with an additional thin ceramic layer to seal the inter-columnar spaces against the

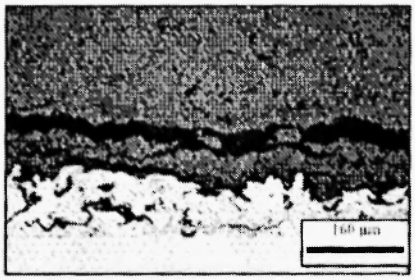

Fig. 6 (c): Micrograpah of as detected partial TBC spallation /40/.

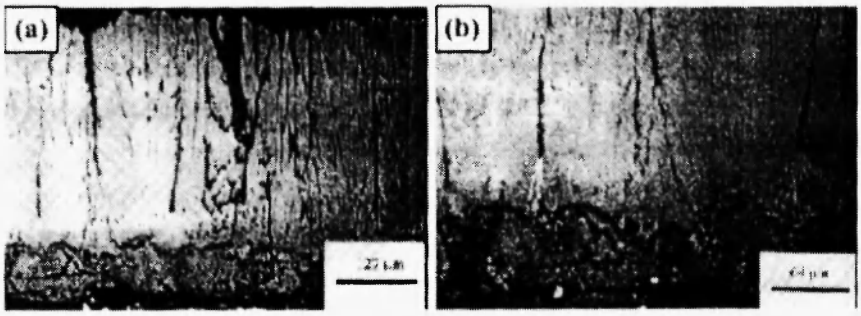

Fig. 6 (a & b): Microstructure at 200× (a) and 400× (b) of EB-PVD 7YSZ ceramic, showing contaminant infiltration to the bond coat after exposure to 1311K for 1000 hours /40/.

penetration of corrodants and sintering agent (Figure 7). The ceramic erosion test is conducted on a coated flat specimen surface at 1366K, using quartz or arizona road dust as particulate erodants. Figure 7 showed the lowest erosion rate /40/.

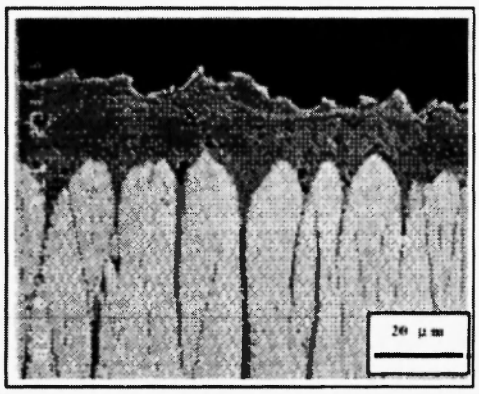

Fig. 7: Typical as-coated microstructure of a surface-modified EB-PVD 7YSZ specimen /40/.

A reduction in chromium content results in loss of hot corrosion resistance of heavy-duty liners, where corrosion may be type I a high temperature (1033-1200K) corrosion at slow rate and type II a lower temperature (1005-1033K) corrosion at faster rate. This corrosion occurs on bare substrate and in the presence of condensed alkali salts /41/.

(4) Modification of thermal barrier coatings:

Modifications in thermal barrier coatings require modification of ceramics, modification of bond coat, microlaminations of ceramic/metallic coatings, and functionally graded materials (FGM).

(4a) Usage of different stabilizer:

Ceria stabilized zirconia is an economical and stable TBC former, when ceria content is greater than 20%. The plasma spray transforms cubic to zt′ phase instead of t or t′. zt′ phase characteristic is similar to t′ phase as found incase of rapid solidification of YSZ. Comparatively smaller grain size and greater volume expansion hysteresis of phase transformation increase high temperature thermomechanical performances of ceria stabilized zirconia /61/.

(4b) Microlaminated thermal barrier coatings:

Yttria stabilized zirconia is the most commonly used topcoat material. Where the underlying bond coat of the MCrAlY family is to improve coating adherence by reducing coefficient of thermal expansion mismatch and allow formation of adherent Al_2O_3 scale. However in order to satisfy the primary purpose of thermal insulation to further increase lifetime and performance, incorporating multiple phases or functionally graded materials (FGM) properly alters the TBC. The multi-layer architecture of ZrO_2 and Al_2O_3 produces a composite system under mutual compensation of volumetric expansion and contraction at high temperature. The transmission electron microscope (TEM) image of interface shows the absence of interlayer porosity and the high degree of bonding (Figure 8). Exposure to temperature-hours has showed absence of delamination in Figure 8. As sprayed 7 wt. YSZ is typically present as metastable t′-ZrO_2. Coating durability has been directly linked to the percentage of this phase. However, t′-ZrO_2 is diffusionally unstable at high temperature and reverts to equilibrium t-ZrO_2. Upon cooling t-ZrO_2 can further transform to the monoclinic phase, resulting in a 4.5% volumetric expansion. In a similar manner, as sprayed γ-Al_2O_3 is unstable at high temperatures. The transformation of γ-Al_2O_3 to α- Al_2O_3 at high temperature results in an 11% volumetric reduction /44/.

(4c) Elemental performances in bond coat:

Elemental introduction into metallic bond coat is studied using different techniques of incorporation and compositions. Y, Zr, Al, Cr, Pt, Pd, Rh, Hf, and Ce

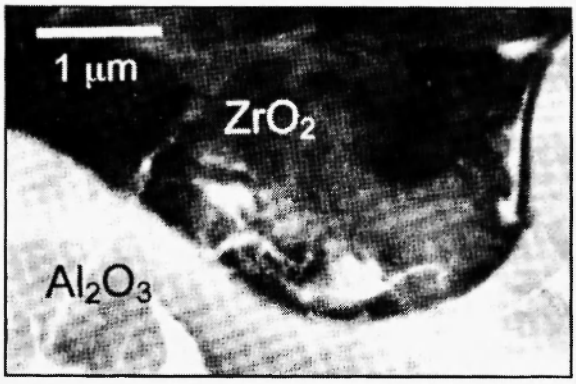

Fig. 8: TEM of an alumina/zirconia interface, which reveals the high degree of interfacial contact. The black lines denote the interface between the alumina and zirconia /44/.

produce improvements, while S, Mn, Ti, Ta, V and halogens form poisoning effects. A lower content of silicon appears to improve performance otherwise a low temperature oxide (equilibrium) eutectic former. Reactivity and diffusion tendency appears to play a key role in the variation of performance /62-67/. Comparing the compositions measured with an isothermal (1333K) section of the ternary phase diagram of (Ni-Al-Pt) shows that the overall composition of the bond coat moves from the single phase β-(Ni, Pt)Al region to a two-phase (β + γ') composition as a result of thermal cycling. This migration to a Ni-rich composition explains the formation of the γ'-Ni_3Al precipitates. This can also be directly related to the martensite transformation studies of Ni-rich binary NiAl that have revealed the formation of a martensite phase by transformation from B2 to L1o upon cooling from temperatures greater than 1373K, for compositions of 61 to 68 at. % Ni. The room temperature composition of the L1o phase is located at the boundary of the β-phase field in the 1333K isotherm. It is clear that the bond coat partition into two phases (β-(Ni,Pt)Al + γ'-Ni_3Al) and that of B2 to L1o transformation occurs in a diffusionless manner /68/.

(5) Non-destructive test on thermal barrier coatings:

The non-destructive test is a valuable examination to assess in service rate of degradation. Experiment within and around service exposure schedule estimates remnant lifetime rationally and increases safety and reliability of service.

(5a) Air flow test:

Two primary failure modes associated with all combustion hardware have been wear of mating surfaces and degradation of TBC system in power sector liners (Table-1). I & RS service centers to assess TBC degradation have recently introduced non-destructive thickness surveys. A critical test also has been implemented for louvered liners. This is called the airflow test. The flow test assures that the combustion liner in the set have been flowing the same amount of air to minimize temperature variances. During test liner is placed on the flow check machine and a vacuum is drawn through the liner. The test machine calculates the effective airflow area and respective derivation of required correction /85/.

(5b) Photoluminescence piezospectroscopy:

Figure 9 shows the experimental setup of spectroscopy. The fiber optic cable attachment allows one to measure thermal barrier coating of variously sized and shaped components /69/. Non-destructive inspection of spallation through interface of ceramic coat and bond coat during service exposure is inevitable. Clarke and co-workers have developed the technique of structural integrity assessment of TBC around TGO layer. The TGO stress signal is measured from Cr^{+3} photoluminescence piezospectroscopy, where Cr^{+3} is used as an impurity in α-alumina rich TGO. The Cr^{+3} photoluminescence in α-alumina occurs by the excitation and subsequent relaxation of chromium ions resulting in photon emission. Two distinct fluorescence transitions are allowed by the crystallographic

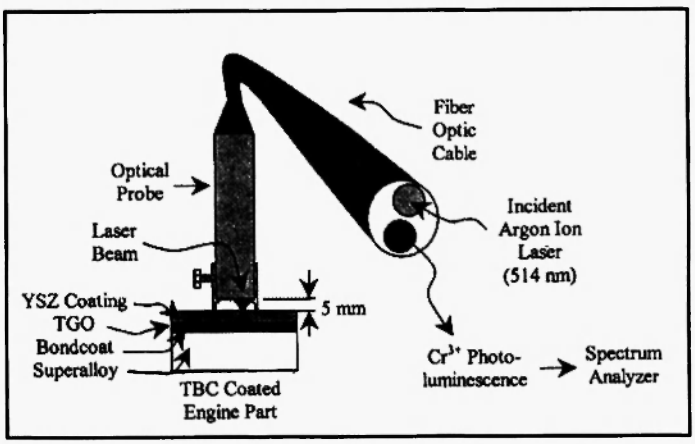

Fig. 9: A schematic diagram of the experimental setup for the Cr^{+3} photoluminescence piezospectroscopy with the extension of fiber optics /69/.

symmetry of the Cr^{+3} site in stress free sapphire crystals corresponding to the R_1 and R_2 fluorescence doublets, occurring at frequencies of 14,402 and 14,432/cm, respectively. A schematic shift in the position of these peaks of strained crystal is known as the piezo-spectroscopic effect. The fluorescence frequency shift $\Delta\gamma$, and the local stress within the sapphire can be phenomenological, related to the coefficients of the piezospectroscopic tensor /69/.

DAMAGE ASSESSMENT AND LIFE PREDICTION OF LINERS

Because of the high cost of tooling in the manufacture of gas turbine engines, there is a great incentive to predict the life of competing designs of turbine parts rather than identifying superior designs through building and testing /54/. An integral part of the evaluation of the merits of different designs prior to developing hardware is based on calculating TBC life for previous operating histories. Accordingly a variety of life-prediction methods have been developed for engineering purposes. The TBC life prediction would be the failure mechanisms for a specific TBC under its relevant engine operating conditions. At present such life prediction is still not practical because of lack of knowledge of the operative mechanism, physical and mechanical properties data as a function of temperature and strain rate for the four layers of the TBC, and lack of quantitative models for some processes, especially oxidation behavior in complex multi-component alloys, and exact conditions under which one mechanism of failure is replaced by another. Progress in understanding the failure mechanism has to be based not only on physical experiments but also on increasingly realistic finite element models of local failure modes. Rapid improvement of the understanding and modeling of specific failure mechanisms characterize the state of the art mostly by academic researchers, whereas the industry continues to use semi-empirical models. In developing semi-empirical models, the two primary goals are (i) to include the correct variables and (ii) to incorporate them in functional forms that provide the best probability of extrapolating current engine experience to future designs where temperatures and other factors may be different. In the model, the primary damage variables chosen are the TGO thickness and mechanical strain range in the TBC. TGO thickness is the most appropriate variable, because it is a measure of stored strain energy and is implicated in most of the damage mechanisms. The use of mechanical strain range captures the idea that larger strain excursions associated with larger temperature excursions are increasingly damaging /70,71/. Semi-empirical models such as this must be calibrated against data to determine a number of empirical parameters. The calibrated version of this model has been successful in predicting failure for the conditions and materials for which it was developed. The ultimate research goal, with respect to life prediction, is to reach a state of knowledge that allows mechanism-base models to be used in engineering practice. In the interim, improvement in the understanding of operative mechanisms allows for more insightful choices of variables, properties, and functional forms in engineering models. The future outlook for improved materials will continue to play a major role in meeting the gas turbine industry's requirement for improved durability and energy efficiency /72/. Implementation of alternate high temperature structural materials such as ceramics, ceramic composites, intermetallics, and refractory metal alloys is still in the developmental stages. The near term focus will be on TBC's with improved durability and performance /54/. Major improvements in both durability and performance should be achievable by using approaches that are based on the recent understanding of TBC failure mechanisms, which are summarized below. The durability of yttria stabilized zirconia based TBC's can be substantially increased with improvements in bond coat composition and processing. The key to durability is the retention of strong bonding between the TGO and bond coat. In order to accomplish this, it is necessary (i) to create and maintain a strong initial bond and (ii) to reduce the stresses and accumulated strain energy that promotes cracking at the bond coat/TGO interface. To create a strong initial bond, it is important that the bond coat composition and the heat-treatment should be such that no other transient oxides except Al_2O_3 is the initial oxide layer that forms on the bond coat, and all bond coat surface defects and roughness should be eliminated

/34/. To maintain a strong bond, the diffusion of deleterious elements such as sulphur, titanium and tantalum from the superalloy substrate or the bond coat to the interface must be prevented during elevated temperature service exposure. Considerable progress has been made in reducing sulphur content in alloys. It is desirable to have a flat interface, and to have a creep resistant bond coat that reduces further interface roughening during cyclic engine operation in both EB-PVD and APS-TBC. It also minimizes the out of plane tensile stresses across the interface and the strain energy contained in the TGO. A four-fold improvement in TBC durability has been achieved by reducing the interfacial roughness /44/. It is also desirable to have a bond coat composition that reduces the growth rate (thickening) of the TGO and promotes adherence of a thicker TGO. In APS-TBC's in addition to the cracking at the bond coat/TGO interface, there is spallation at the topcoat splat boundaries. Toughening or eliminating these splat boundaries will increase APS-TBC durability. This has been achieved by using an innovative plasma spray process. Segmented topcoats with periodic cracks normal to the metal/ceramic interface are desirable for increasing the strain tolerance in APS-TBC's /44,52,73/. A TBC with this feature has been implemented commercially. Suppression of sintering within the topcoat (in both EB-PVD and APS-TBC) at operating temperatures is also desirable for maintaining high strain tolerance /17/. There are great motivations for developing ceramic topcoats with reduced high temperature thermal conductivity. Reduced thermal conductivity will help to (i) improve TBC durability by reducing the metal temperature and retarding the thermal activity process responsible for failure and/or (ii) improve engine efficiency by allowing it to operate at higher temperatures. To reduce thermal conductivity at elevated temperature, it is necessary to reduce phonon conduction and radiated heat transfer. Choosing new ceramic containing high concentrations of point defects, such as oxygen vacancies and solute atoms with a high atomic weight relative to the host that can reduce phonon conduction. Rare earth zirconates are examples of such ceramics now under consideration for use as TBC's. Use of suitable reflective coatings may reduce radiation. Strategic placement of oriented cracks and pores within the topcoat and suppression of sintering at operating temperatures will also reduce both phonon conduction and radiative heat-transfer. In the search for suitable new TBC ceramics, success will ultimately come from a fuller appreciation of the favorable characteristics that have made YSZ such a successful TBC to date, and the incorporation of these characteristics in a ceramic with lower conductivity and higher temperature /70/. Satisfactory lifing methodology and attractive rationale for coating life time prediction can be referred with confidence ensuring that the strain energy release rate at interface remains below the fracture energy of the interface. The relatively high mechanical stability of plasma sprayed zirconia topcoats is due to low macroscopic stiffness, which ensures low residual stress levels and the material has a high strain tolerance. Under service conditions the stiffness of topcoat rises as defects (microcracks, pores, and lack of intersplat bonding) start to sinter and heal. This raises residual stress levels and associated strain energy release rate, making spallation more likely. Heat-treatment of air plasma sprayed zirconia increases stiffness proportional to the temperature. The associated grain growth, improvement in bonding, and coherence across splat boundaries increase stiffness. However, the rise of stiffness can be divided into two regimes, a rapid initial increase, followed by a more progressive rise (above 1473K). Eaton and Novak have observed sharp changes in stiffness after short sintering time /40/. The detectable effects in plasma sprayed zirconia below 1073K have been reported by Wesling *et al.* Free surface and heat-treatment temperatures below 1673K have showed no such comparison of stiffening. Treatment with corrodant and sintering agent does not affect the property more than the contamination free state /40/.

Microstructural changes in coated turbine blades during service have been predicted by DICTRA software. This technique is illustrated by calculating the microstructures that will form between a nickel base $\gamma + \gamma'$ alloy and MCrAlY type $\beta + \gamma$ alloys. It is shown that a number of different microstructures can form initially, depending on the coating composition. As the ceramic composition of the coating varies during service, the microstructure may change several times. These variations can be illustrated on an "Interdiffusion Microstructure Map".

The following life prediction model describes the tools for reduction of engine design risk and overhaul requirement of hot section components. The preliminary TBC life prediction has been based on measurement of material property such as (1) Thermal expansion and material properties for all four components, that is substrate, bond coat, ceramics, and thermally grown oxides (TGO), (2) Corrosion properties of bond coat, ceramics, and TGO, (3) Sintering properties of ceramics, and TGO, (4) Phase transformation and contamination involved for respectively ceramics, and TGO. The contamination property is inspected after measurements of TGO thickness, defects, and structure, and the growth stress involved is judged from TGO structure, and TGO-bond coat interfacial topography. Further the TBC life is derived from the TBC strength /82/. Benefits of destructive test characteristics to identify assessment parameters have to be considered for rejuvenation and life extension. The information may be as follows. (a) Establishment of possible sources of contamination from chemical analysis of corrosion products; (b) Difference of internal and external cooling hole microstructure; (c) Assessment of service temperature from coarsening of γ', and diffusion zone growth of components; (d) Study of difference in existence of crack location, frequency, and penetration; and (f) Arrangement of irreparable items in time to maximize availability of replacement /41,51/.

CURRENT SCENARIO OF COMBUSTOR LINERS

Corning has retrofitted hot section components with ceramics. Improvements achieved have been better performance, lower emission, and greater temperature durability. Since they are elastic flow insensitive, even the 762-mm diameter outer combustor liner can be fabricated in one piece, because hot wall combustor liners are generally exposed to only minimal mechanical stresses. Continuous Fiber Ceramic Composite (CFCC's) are emerging as strong contenders for the combustor application. CFCC's liners for this application are being analyzed, designed, and fabricated under the DOE-sponsored ceramic stationary gas turbine (CSGT) program /74/. In the recent configuration CFCC's are to replace a 203-mm long cylindrical portion of the 330 mm diameter inner volume and 762-mm diameter outer wall of the combustor. CFCC's potentially offer many advantages in the combustor application. Also, their toughness gives them the ability to withstand impacts during handling, assembly, and operation. Another advantage of CFCC's is that turbines tend to become non-catastrophic. It minimizes spalling or separation of large pieces and the potential for damaging monolithic ceramic and/or metallic part downstream. Finally CFCC's have the high temperature capability needed to endure the target turbine rotor inlet temperature of 1394K. A two-cylinder metallic combustor and a cylindrical CFCC combustor have been tested at typical gas turbine operating conditions in a sub-scale test rig. The same natural premix fuel injector has been used for all of the testing. These metallic combustors differ in the amount of cooling air used to maintain acceptable liner temperature. A conventional louver cooled liner uses the most liner cooling air. An effusion-cooled liner uses less cooling air. Only backside cooling is used with the ceramic liner. At given NO_x level the metal liners show high CO levels than the ceramic liner. This is attributed to the quenching effect of the liner cooling air. With no cooling air injection, the ceramic combustor produces NO_x levels below 10 ppm with low CO emissions. Two metallic liners are limited to NO_x emissions near 20 ppm without producing excessive CO. Full scale 3D woven SiC/SiC liners and alumina/alumina are completely successful /49/.

High performance low emission engine systems lead to a significant improvement in local air quality, minimum impact on ozone depletion and level to an overall reduction in aviation contribution to global warning /43/.

The developed techniques have contributed to reduction of NO_x by 70% at take off and landing and overall fuel savings of 8-15%. Substitutive application of ceramic matrix composites (CMC) are studied for combustor liner and turbine vanes, advanced disc alloys, turbine blade material system, whereas high temperature polymer matrix composite and innovative light materials are studied for static engine structure.

Several high-temperature ceramic materials are under development, allowing realizations of higher

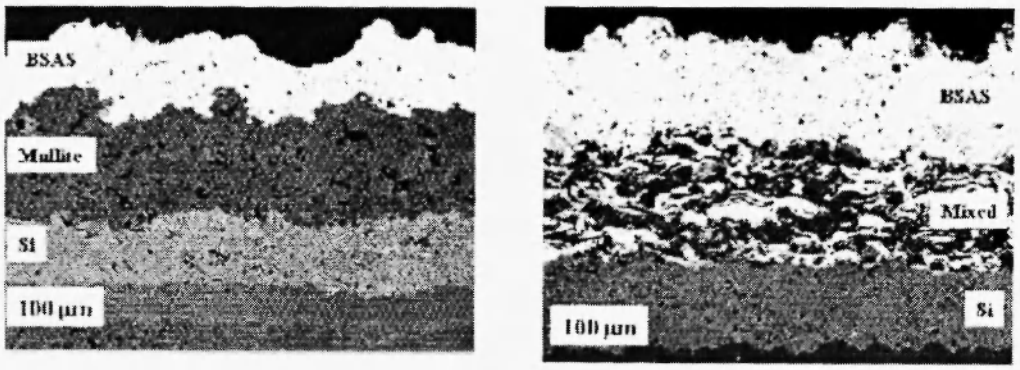

Fig. 10: Microstructure of EBC as deposited on MI SiC/SiC composite (dual layer of mullite/ BSAS and mixed layer of mullite+BSAS/ BSAS /36/.

efficiency, lower emission gas turbines. These materials include SiC/SiC composites, oxide/oxide composites, environmental barrier coatings (EBCs) (SiN_3), and TBCs (YSZ). Plasma sprayed coatings consist of two layers on a silicon bond coat and chemical vapour deposition (CVD) SiC seal coat (Figure 10). Ceramic matrix composite has been developed for supersonic gas turbine combustor liner. The material is a silicon carbide fiber composite in a silicon carbide matrix. The fiber improves fracture toughness. The estimated operating goal for liner material is 9000 hours at 1483K. However silicon carbide reacts with combustion products at operating temperatures. An environmental barrier coating system has been developed to improve surface recession resistance of the material system and to increase the hot side temperature capability to 1533K. Optimized fiber architecture processes from Sylramic to Hi-Nicalon meet the performance goals of advanced combustor liners. The TBC-EBC system of coatings over vanes operates at temperature of 1672K with a marginal reduction of temperature by 422K /75/. Ceramic combustor addresses the CO quenching issue in the same manner as the ABC liner. Cooling air injection through the liner is avoided to provide potential emission benefits. The emission benefits have been found to be very similar to those of the ABC liners /1/.

Non-destructive inspection (NDE) technology has been developed to reduce risk of failure of ceramic components of gas turbines. Inspection before and after application of EBCs on hot wall ceramic combustor liner in response to delaminations, condition of outages, seams, splits, and loss of properties has been done successfully using NDE. This technique approach is based on spectrally tuned flash infrared imaging for a through transmission from one side. The technique has been non-contact, non-invasive, requires no water coupling for ultrasonic, and has provisions of on-offi engine examination. The thermal imaging NDE experimental approach utilizes the effect of optical properties or Parker's theory of surface temperature decay. The theory assumes that the material is heated with a step heating pulse whose penetration depth is negligible. In cases where absorption depth cannot be considered negligible for translucent materials, the conventional diffusivity difference is indicated by an infrared coloration for lower diffusivity/flawed zone and blue coloration for greater diffusivity/normal zone /36/.

CONCLUSIONS

The combustor liner has been reevaluated by changes in its construction within existing design. The thermal profiles of engines produce a variety of temperature and load variation consequences. The light weight philosophy of combustion engine components on the other hand has improved liner durability by a variety of thermal barrier coating (TBC) systems. Cooling air, ceramic coating, and combustion catalysts lower liner temperature. Liner life is therefore increased many times more than with the older state of the art. The low NO_x premix dry combustion helps to combat pollution problems.

Aging and TGO formation in TBC cause failure of ceramic coating by topcoat sintering and bond coat elemental depletion. Both effects mitigate the mismatched stress at interface by spallation, buckling, and delamination of coating. Subsequent high temperature corrosion of substrate damages the liner metal.

Application of Functionally Graded Materials (FGM), and Environmental Barrier Coating (EBC) with Thermal Barrier Coating (TBC) improves performance as compared to Thermal Barrier Coating (TBC) alone. On the other hand replacement of metallic liners by ceramic liners provide new avenues for the state of art in modern trend.

Conventional designs of combustion chamber liner in different capacity of performance have been uprated by introduction of advanced material application. Refractory metal, ceramics, cermets and intermetallic compounds have emphasized in this respect.

REFERENCES

1. L. Witherspoon and L. Cowell. Solar Turbines Incorporated, 9330 Sky Park Court, MZ. SP3-Q, San Diego, CA 92123-5398. Next generation Dry Low NOx for gas turbines. Environmental and Regulatory impact (2002) (http://www.gmrc.org/gmrc/tech papers PDF/2002/ next_ generation_dry_low.pdf).
2. H. Cohen, G.F.C. Rogers and H.I.H. Saravana-muttoo (Ed.). *Gas Turbine Theory*, 4th edition, and book chapter, 233-267 (1996).
3. A. Bennett. Properties of thermal barrier coatings, *Mater. Sci. & Technol.*, **2**, 257-261, March (1986).
4. H. Herman and S. Sampath. Thermal spray coatings, Book chapter, *Metallurgy and Ceramic Protective Coatings*, Ed. Kurt H. Stern, Chapman and Hall, London, chap.10, 261-289 (1996).
5. J.L. Cocking, P.G. Richards and G.R. Johnston. Comparative durability of six coating systems on first stage gas turbine blades in the engines of a long-range maritime patrol air craft, *Surface and Coatings Tech.*, **36**, 37-47 (1988).
6. W.D. Grossklaus, G.B. Katz, and D.J. Wortman. Performance comparison of advanced airfoil coatings in marine service, Book chapter, High temperature coatings, Ed. M. Khobaile, R.C. Krutena, A publication of the Mater. Soc. Inc., Pennsylvania, 67-83 (1987).
7. U. Schulz, and M. Schmucker. Microstructure of ZrO_2 thermal barrier coatings applied by EB-PVD, *Mater. Sci. and Eng. A*, **276** (1-2), 1-8, 15 Jan. (2000).
8. M.J. Stiger, N.M. Yanar, M.G. Topping, F.S. Pettit, and G.H. Meier. Thermal barrier coatings for the 21st century, *Z. Metallkd.*, **90**, 1069-1078 (1999).
9. R. Sivakumar, and B.L. Mordike. High temperature coatings for gas turbine blades, A review, *Surface and Coatings Tech.*, **37**, 139-160 (1989).
10. P.D. Harmsworth, and R. Stevens. Microstructure of zirconia-yttria plasma-sprayed thermal barrier coatings, *J. Mater. Sci.*, **27**, 616-624 (1992).
11. R.C. Wu and E. Chang. Microstructure, properties and failure analysis of (ZrO_2-8wt. %Y_2O_3)/((Co, Ni)-Cr-Al-Y) thermal barrier coatings, *Mater. Sci. and Eng.*, *A***111**, 201-210 (1989).
12. L. Lalit, S. Alperine, C. Diot and M. Mevrel. Thermal barrier coatings. microstructural investigation after annealing, *Mater. Sci. Eng.(A)*, 120-121, 475-482 (1989).
13. C. Leyens, U. Schulz, K. Fritscher, M. Bartsch, M. Peters and W.A. Kaysser. Contemporary Materials Issues for Advanced EB-PVD Thermal Barrier Coating Systems, *Zeitschrift fur Metallkunde*, **92** (7), 762-772, July (2001).
14. J.A. Thompson and T.W. Clyne. Stiffness of plasma sprayed zirconia topcoats in TBCs, *United Thermal Spray Conference*, 835-840, March (1999).
15. Y. Itoh, T. Kameda, T. Okamura and K. Nagata. Sintering behavior of zirconia thermal barrier coating under gradient temperature, *Journal of the Society of Materials Science, Japan*, **48** (7), 740-745, July (1999).
16. C.C. Berndt. Failure processes within ceramic coatings at high temperatures, *J. Mater. Sci.*, **24**, 3511-3520 (1989).
17. V. Provenzano, K. Sadananda, N.P. Louat and J.R. Reed. Void formation and suppression during high

temperature oxidation of MCrAlY-type coatings, *Surface and Coatings Tech.*, **36**, 61-74 (1988).

18. M.Y. Ali, X .Chen and G.M. Newaz. Oxide layer development under thermal cycling and its role on damage evolution and spallation in TBC system, *J. of Mater. Sci.*, 36, 4535-4542 (2001).
19. C. Burman, T. Ericsson, I. Kvernes and Y. Lindblom. A comparison between different compounds for improving the corrosion protection of FeCrAlY coatings on superalloys, *Surface and Coatings Tech.*, **36**, 1-12 (1988).
20. W. Brandle, H.J. Grabke, D. Toma and J. Krueger. The oxidation behavior of sprayed MCrAlY coatings, *Surface Coat Tech.*, **86-87**, 41-47 (1996).
21. T.M. Yennshonis. Overview of thermal barrier coatings in diesel engines, *J. of Thermal Spray Technology*, 6(1), 50-56 (1997).
22. B.J. Gill and R.C. Tucker. Plasma spray coating processes, *Mater. Sci. & Technol.*, **2**, 207-213, March (1986).
23. P.D. Harmsworth and R. Stevens. Phase composition and properties of plasma-sprayed zirconia thermal barrier coatings, *J. Mater. Sci.*, **27**, 611-615 (1992).
24. B.C. Wu, E. Chang, R. Tu and S.L.Wang. Microstructures, properties and failure analysis of (ZrO_2-8wt.%Y_2O_3)/(Co,Ni)-Cr-Al-Y) thermal barrier coatings, *Mater. Sci. and Eng. A*, **A111**, 201-210 (1989).
25. A.K. Ray, N. Roy and K.M. Godiwalla. Crack propagation studies and bond coat properties in thermal barrier coatings under bending, *Bulletin of Materials Science (India)*, **24** (2), 203-209, April (2001).
26. B. Hics. High temperature sheet materials for gas turbine applications, *Mater. Sci and Technol.*, **3**(9), 772-781 (1987).
27. D. Zhu and R.A. Miller. Investigation of thermal high cycle and low cycle fatigue mechanisms of thick thermal barrier coatings, NASA, Tech. Memo. 1998-206633.
28. J.K. Tien and F.S. Pettit. Mechanism of oxide adherence on Fe-25Cr-4Al (Y or Sc) alloys, *Metall. Trans.*, 3, 1587-1599, June (1972).
29. A. Atkinson and R. Guppy. Measurement of adhesion of oxides grown on nickel and nickel alloys, *Mater. Sci. & Technol.*, 7, 1031-1041, Nov. (1991).
30. E. Lopez, F. Beltzung and G. Zambelli. Measurement of cohesion and adhesion strengths in alumina coatings produced by flame spraying, *J. of Mater. Sci. Lett.*, **8**, 346-348 (1989).
31. A.W. Funkenbusch, J.G. Smeggil and N.S. Bornstein. Reactive element sulphur interaction and oxide scale adherence, *Metall. Trans. A*, **16A**, 1964-1965, June (1985).
32. James L. Smialek. Adherent Al_2O_3 scales formed on undoped NiCrAl alloys, *Metall. Trans.*, **18A**, 164-167, Jan. (1987).
33. V.K. Tolpygo, D.R. Clarke and K. S. Murphy. The effect of grit blasting on the oxidation behavior of a platinum-modified Ni-aluminide coating, *Metall. and Mater. Trans. A*, **32A**, 1467-1478, June (2001).
34. D.W. Esbeck, I.S. Gates and P.H. Schneider. Industrial advanced turbine systems program overview, Research sponsored by U.S.Dept. of energy's Morgantown energy technology center and Chicago operations office with solar turbines (Sandiago) (1997) (http//www.netl.doc.gov/ publications/proceedings/97/97ats/ats_pdf/ATS2-2.PDF).
35. Kesri M. Godiwalla, Nilima Roy, Satyabrata Choudhury and Asok K Ray. Investigation and modeling of mechanical properties for thermal barrier coatings under bonding, *Int. J. of Turbo and Jet Engines*, **18**, 77-103 (2001).
36. W.A. Ellingson, J.G. Sun, C. Deemer, R. Visher and E.R. Koehl. NDE technology for risk reduction of ceramic components for gas turbines, Argonne National Laboratory, Argonne, IL, USA, First International conference on gas turbine technologies, Brussels, Belgium (10-11th July 2003), http://www.came-gt.com/Internat conf/ presentations/Session4-Fri-am/mat%2001%20 Ellingson.pdf.
37. The GE90-An Introduction, http://www.anirudh.net/seminar/ge90./pdf
38. W. Endres. Design principles of gas turbines, Ed. P.R.Sahm and M.O.Speidel. High-temperature materials in gas turbines, *Proceedings of symposium on High-temperature materials in gas*

turbines, Brown, Bovery & Co. Ltd., Baden, Switzerland, 1973, Book chapter 1, 1-14 (1974).

39. Alan S. Feitelberg, Melvin R. Jackson, Michael A. Lacey, Kenneth S. Manning and Ann M. Ritter. Design and performance of a low Btu fuel rich-quench-lean gas turbine combustor, GE corporate Research and Development, PO. Box 8, Schenectady, NY 12301, http://www.netl.doe.gov/publications/proceedings/96/96ps/ps_pdf/96ps1_7.pdf.
40. Mladen E. Trubelja, David M. Nissley, Norman S. Bornstein and Jeanine T.D. Marcin. Pratt & Whitney thermal barrier coating development, Research sponsored by the U.S. Department of Energy's Oak Ridge Operations office under Contract No. DE-AC05-95OR22426 with Pratt & Whitney, 400 Main street, M/S 114-41, East Hartford, CT 06108, Phone No.(860)565-4784, Telex No. (860) 565-5635, E-mail. marcinj@pwch.com.
41. K.J.Pallos. Gas turbine repair technology, GE Power systems, GER-3957b, GE energy services technology, Atlanta, GA, http://www.gepower.com/prod_serv/products/tech_docs/en/downloads/ger 3957b.pdf.
42. Y. Tsukuda, E. Akita, Y. Iwasaki, K. Yanou, Y. Kawata, T. Noguchi and Toshihida Noguchi. Higashi Niigata thermal power station operating status, 1450 class gas turbine operation, Mitsubishi Heavy Industries limited, *Technol. Review*, **38**, No.3, Oct. (2001) (http:/www.mhi.co.jp/tech/pdf/e383/p101.pdf).
43. Ashok K. Ray. Failure mode of thermal barrier coatings for gas turbine vanes under bending, *Int. J. of Turbo and Jet Engines*, **17**, 1-24 (2000).
44. Y. Jennifer Su, Hsin Wang, Wally D. Porter, A.R. De Arellano Lopez and K.T. Faber. Thermal conductivity and phase evolution of plasma spread multilayer coatings, *J.of Mater. Sci.*, **36**, 3511-3518 (2001).
45. A. Rabiel and A.G. Evans. Failure mechanisms associated with the thermally grown oxide in plasma-sprayed thermal barrier coatings, *Acta Mater.*, **48**, 3963-3976 (2000).
46. J.L. Pierce, L.P. Zawada and R. Srinivasan. Tensile behavior of SiC/C and Rene-41 following isothermal exposure and thermal fatigue, *J. Mater. Sci.*, **35** (12), 2973-2984, 15th June (2000).
47. Nitin P. Padture, I Maurice Gell, I. Eric and H. Jordan. Thermal barrier coatings for gas turbine engine applications, *Review. Mater. Sci.*, **296**, 280-284, 12 April (2002) (http://www.ims.uconn.edu/metal/faculty/Padture Papers/Padture,TBC Science.pdf).
48. Dimitri N. Mavris and Bryce Roth. A methodology for robust design of impingement cooled HSCT combustor liner, *American Institute of Aeronautics and Astronautics, 35th Aerospace Sciences Meeting and Exhibition*, 6-9 January (1997) (http://www.asdl.gatech.edu/publications/pdf/1997/AIAA-97-0288.pdf).
49. Steve DiPietro. Communication of the continuous fiber ceramic composite program, USA, Dept. of Energy, CFCC News, Summer (1995), No.6 (http://www.hsrd.ornl.gov/cfcc/cfcc_nc.pdf).
50. Jennifer E Gill. Uprate options for the MS900A heavy-duty gas turbine, GE Power Systems Schenectady (http:/www.gepower.com/publications/en ns/pdf/ger 3928a.pdf).
51. Udaya Rao. DOE high efficiency engines and turbines (HEET) materials roadmap, DoD-NASA-DOE-FAA Alliance workshop #7 on Propulsion and Power Systems, National Energy Technology Laboratory, 2nd May (2002).
52. A.K. Ray and R.W. Stinbreach. Thermo-mechanical characterisation and modeling of ceramics and coatings in power plant applications, Internal report of (INDO-GERMAN) collaborative project IN-283 (1998), IWE-1, Julich, Germany.
53. T. Tomimatsu, Y. Kagawa and S.J. Zhu. Residual stress distribution in electron beam-physical vapour deposited ZrO_2 thermal barrier coating layer, *Metall. and Mater. Trans.*, **34A**, 1739, August (2003).
54. K. Yasuda and H. Takeda. Phase transformation during alternating aging at 473 K and at 773 K in the plasma-sprayed yttria stabilized zirconia coating, *J. Mater. Sci.*, **35**, 4379-4383 (2000).
55. Robert Siegel and M. Spuckler Charles. Analysis of thermal radiation effects on temperatures in turbine engine thermal barrier coatings, NASA

Tech. Reports, Document ID.-19980219328, 1st Jan. (1997) (E-mail. help@sti,nasa.gov).

56. Robert Siegel. Thermal radiation effects analyzed in translucent composite and thermal barrier coating, NASA Gleen's research and technology reports, May (1997) (E-mail. Walter.S.kim@grc.nasa.gov).
57. K.L. Choy, J. Mei, J.P. Feist and A.L. Heyes. Microstructure and thermoluminescent properties of ESAVD produced Eu doped Y_2O_3-ZrO_2 coatings, *Surface Engineering*, **16**, No. 6, 469-472 (2000).
58. E.D. Honders, M.P. Seah, S. Hefmann and P. Lejcek. *Interfacial and surface microchemistry*, 4th Ed. Robert W Cahn and Peter Haasen. Physical Metallurgy, Book chapter, No. 13, 2, 1263 (1996).
59. B. Baufeld, E. Tzimas, P. Hahner, H. Mullejans, S.D. Peteves and P. Moretto. Phase angle effects on damage mechanisms of thermal barrier coatings under thermomechanical fatigue, *Scripta. Meter.*, **45**, 859-865 (2001).
60. M. Chatterjee, J. Ray, A. Chatterjee, D. Ganguli, S.V. Joshi and M.P. Srivastava. Thermal barrier coatings from sol-gel derived spray grade Y_2O_3-ZrO_2 microspheres, *J. Mater. Sci.*, **28**, 2803-2807 (1983).
61. P.D. Harmaworth and R. Stevens. Microstructure and phase composition of ZrO_2-CeO_2 thermal barrier coatings, *J. Mater. Sci.* **26**, 3991-3995 (1991).
62. J.G. Smeggil, A.J. Shuskus, C.T. Burilla and R.J. Cipolli. Use of ion implantation techniques to characterize the oxidation of elemental nickel, *Surface and Coatings Tech.*, **36**, 27-36 (1988).
63. R.E. Malush, P. Deb and D.H. Boone. Structure and 900^0 C hot corrosion behavior of chromium-modified platinum aluminide coatings, *Surface and Coatings Tech.*, **36**, 13-26 (1988).
64. D. Wang. Corrosion behavior of chromized and/ or aluminized 2 ¼ Cr -1 Mo steel in medium- BTU coals gassifier environments, *Surface and Coatings Tech.*, **36**, 49-60 (1988).
65. B.C.Wu, C.H.Chao and E.Chang, L.C.Chang. Effects of bond coat pre-aluminising treatment on the properties of ZrO_2-8wt. %Y_2O_3/Co-29Cr-6Al-1Y thermal barrier coatings, *Mater. Sci. & Eng.*, **A124**, 215-221 (1990).
66. J.L. Cocking, J.A. Sprague and J.R. Reed. Oxidation behavior of ion implanted NiCrAl, *Surface and Coatings Tech.*, **36**, 133-142 (1988).
67. Y. Zhang, J.A. Haynes, W.U. Lee, I.G. Wright, B.A. Pint, K.M. Cooley and P.K. Liaw. Effects of platinum incorporation on the isothermal oxidation behavior of chemically vapour deposition aluminide coatings, *Metall. and Mater. Trans. A*, **32A**, 1727-1741, July (2001).
68. M.W. Chen, K.J.T. Livi, P.K. Wright and K.J. Hemker. Microstructural characterisation of platinum modified diffusion aluminide bond coat for thermal barrier coatings, *Metall. and Mater. Trans.*, **34A**, 2289-2299, October (2003).
69. Y.H. Sohn, K. Schlichting, K. Valdyanathan, E. Jordan and M. Gell. Non-destructive evaluation of residual stress for thermal barrier coated turbine blades by Cr^{3+} photoluminescence piezo-spectroscopy, *Metall. and Mater. Trans.A*, **31A**, 2388-2391, Sept. (2000).
70. S.C. Gill and T.W. Clyne. Stress distributions and material response in thermal spraying of metallic and ceramic deposits, *Metall. Trans. B*, **21B**, 377-385 (1990).
71. J. Matejicke, S. Sampath, P.C. Brand and H.J. Prask. Quenching, thermal and residual stresses in plasma sprayed deposits, NiCrAlY and YSZ coatings, *Acta Mater.*, **47**, No. 2, 607-617 (1999).
72. J.A. Thompson and T.W. Clyne. The effect of heat-treatment on the stiffness of zirconia topcoats in plasma sprayed TBC's, *Acta Mater.*. **49**, 1565-1575 (2001).
73. Asok K. Ray and Rolf W. Steinbrech. Crack propagation studies of thermal barrier coatings under bending, *J. of European Ceram. Society*, **19**, 2097-2109 (1999).
74. Gray Davis, Avtar Bining and Mike Betham. Environmentally preferred advanced generation durability of catalytic combustion systems, Appendix II, RAMD Testing and control system development, November-(2001), California Energy Commission (http:/www.energy.ca.gov/ reports/500-02-040F/APPENDIX_II_RAMD_ TESTING.PDF)

75. K.N. Lee, D.S. Fox, J.L. Eldridge, D. Zhu, R.C. Robinson, N.P. Bansalans and R.A. Miller. Upper temperature limits of environmental barrier coatings based on mullite and BSAS, NASA/TM-2002-211372 (2002).